Implementation of Ionospheric Calibration in BBS

Maaijke Mevius

Version 0.1, March 24, 2009

Contents

1 Introduction

This document gives a description of the current implementation of ionospheric calibration in BBS. The results and the steps taken to come to these results of the ionospheric calibration on WSRT data will also be discussed.
The phase-effect of the ionosphere on a radio-interferometer is an *image-plane* effect, which means that the phase errors for different antenna's depend on the viewing direction. A simple self calibration approach will not be sufficient for large baselines and large beams as is the case for LOFAR. One could solve for phases in the direction of every known source, but of course this would lead to too many parameters and would not solve the problem of interpolation in between sources. We developed an algorithm that connects the phase errors in different regions via a so called Minimal Ionospheric Model (MIM)[2]. The used approach will be discussed below.

1.1 Phase delay

The current implementation only deals with the relative measurement of the phase delays. Other effects for which an absolute measurement of the thickness of the ionospheric layer is required, like Faraday rotation, will not be discussed in this document.
The thickness of the ionosphere is measured in Total Electron Content Units (TECU). TEC is the total number of electrons present along a path between two points: $1TECU = 10^{16}electrons/m^2$. Typically the thickness of the ionosphere varies between 5 and 50 TECU, with small values during the night and the larger values during daytime.
To get the phase delays, we use the following conversion formula:

$$\Delta\phi = 25 \cdot c \cdot \lambda \cdot TEC \tag{1}$$

1.2 Thin screen approach

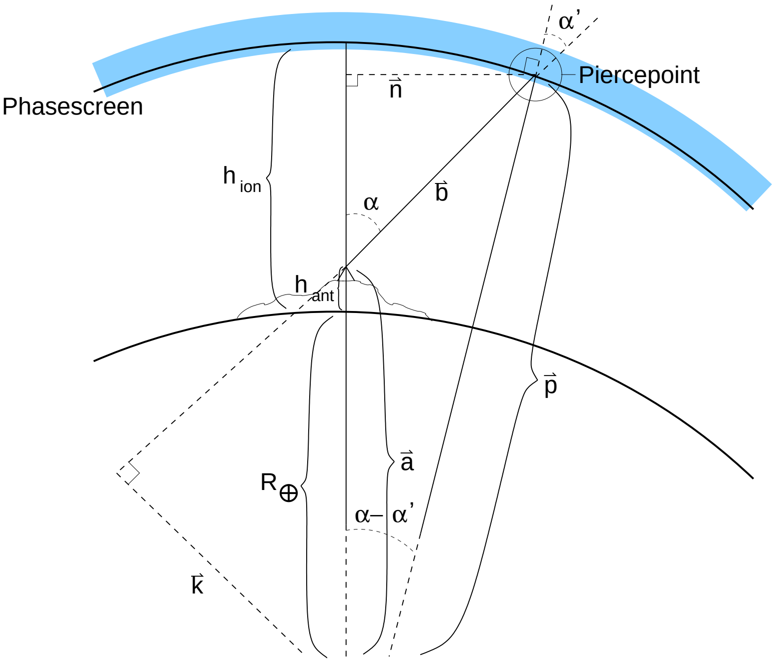

Figure 1: Schematic drawing of pierce-points.

To model the ionosphere we use a thin phase screen at a fixed altitude (currently fixed at 400 km). The crossing points (*pierce-points*) of the lines of sight with this layer can be calculated by simple geometric considerations, see Figure 1. First we calculate angle α'. Since $sin\alpha = \frac{|\vec{k}|}{|\vec{a}|}$, and $sin\alpha' = \frac{|\vec{k}|}{|\vec{p}|}$,

$$\alpha' = asin(sin(\alpha) \cdot \frac{|\vec{a}|}{|\vec{p}|}). \tag{2}$$

Notice that $|\vec{p}|$ is the earth radius plus the fixed altitude of our phase screen (h_{ion}),$|\vec{a}|$ is the earth radius plus the height of the position of the antenna and α is $\frac{1}{2}\pi - elevation$. The relative path length through the ionosphere becomes larger for lower elevations. This can be taken in to account by correcting the TEC-values with:

$$TEC' = TEC \cdot \frac{1}{cos\alpha'}. \tag{3}$$

To get the coordinates of the pierce-point ($\vec{p}$) we need to add $\vec{b}$ to the coordinates of the antenna ($\vec{a}$). We can write the direction of $\vec{b}$ in local *east north up* (ENU) coordinates in terms of azimuth (az) and elevation (el):

$$\frac{\vec{b}}{|\vec{b}|} = \begin{pmatrix} sin(az) \cdot cos(el) \\ cos(az) \cdot cos(el) \\ sin(el) \end{pmatrix} \tag{4}$$

To transform this vector to earth centered coordinates we multiply with the following rotation matrix, with lon, lat the longitude and latitude of the antenna position, respectively:

$$R = \begin{pmatrix} -sin(lon) & -sin(lat) \cdot cos(lon) & cos(lat) \cdot cos(lon) \\ cos(lon) & -sin(lat) \cdot sin(lon) & cos(lat) \cdot sin(lon) \\ 0 & cos(lat) & sin(lat) \end{pmatrix} \tag{5}$$

The length of $\vec{b}$ is:

$$|\vec{b}| = \frac{|\vec{n}|}{sin\alpha}, \tag{6}$$

and:

$$|\vec{n}| = |\vec{p}| \cdot sin(\alpha - \alpha'). \tag{7}$$

This gives for $\vec{p}$:

$$\vec{p} = \vec{a} + R \cdot \begin{pmatrix} sin(az) \cdot cos(el) \\ cos(az) \cdot cos(el) \\ sin(el) \end{pmatrix} \cdot |\vec{p}| \cdot \frac{\sin(\alpha - \alpha')}{sin\alpha} \tag{8}$$

Now, our model of the ionosphere is a function of the pierce-point coordinates. To simplify matters, instead of using earth centered coordinates, we rotate our reference frame to the local ENU coordinates at the position of a reference antenna (usually that of the first antenna). For this we use the inverse of the matrix in equation 5. At the moment, the coordinates on which we span our ionospheric model, are just the x,y coordinates of the pierce points after rotation to the reference frame. This is similar to what is done in SPAM [1]. However, a simple transformation is needed to convert these to the more correct longitude and latitude.

The simple model currently implemented, is just a polynomial of the pierce-point coordinates:

$$TEC = c_{01} \cdot y + c_{10} \cdot x + c_{11} \cdot x \cdot y + \ldots \tag{9}$$

Since we are only interested in the relative phase errors, there is no constant factor c_{00}[1].

1.3 Peeling vs. direct fit

In contrast to other methods ([1]), we fit the ionospheric parameters directly on the uv-data. Intema in his SPAM method, first determines the phase errors in the directions of several strong sources using a peeling scheme[3]. Then he calculates the pierce-points and fits a his ionospheric model on the fitted phases. In BBS we directly and simultaneously apply the phase errors from our ionospheric model and equation 1, to all sources in our sky model (or at least all selected sources). We then minimize the difference of the uv-data with the predicted model by adjusting the parameters of the ionospheric model ($c_{01}, c_{10,...}$ in equation 9). The advantage of the latter method is that it requires less processing steps, and it fits nicely in the general scheme of BBS, which was designed to solve on uv-data. The disadvantage is that the whole fitting process is less transparent and could lead to unwanted instabilities.

1.4 Extensions

Here we suggest some improvements that still remain to be done.

1.4.1 Improving the model

The currently implemented polynomial model has proven to be functional for small arrays like WSRT (see section 3.1). However, we expect this model to fail for larger areas, since it is well known the polynomials show unwanted/unphysical effects at the edges. For a first order determination of the gradient over the field of view, the polynomial model could be very useful. If there are enough bright sources in the field of view and the behavior of the ionosphere is stable enough, a gradient model could be sufficient to determine the *phase ambiguities* of 2π.

A more elaborate scheme that we would suggest is to first remove the phase ambiguities by fitting a low order polynomial phase screen and then fit a more sophisticated model (eg. a model on Karhunen-Loeéve basis, see [1]) with the restriction that the phases lie between $-\pi$ and π. For longer baselines it might be necessary to include more layers at different altitude in the model (the *2.5 D models*).

Also at some point it would be good to investigate time coherency, and implement some sort of time dependence in the models.

1.4.2 Plotting

To investigate the results a 2 dimensional plot (longitude, latitude) of the model in phases or TEC would be helpful. This could probably easily be accomplished by some python script that extracts the MIM parameters from the parmdb and translates them

[1] Note, however, that a fit of the (approximate) absolute TEC values (c_{00}) might be possible if we are able to measure the $1/cos\alpha$ effect as given in equation 3. For this, one probably needs phases over a large field of view and a stable ionosphere.

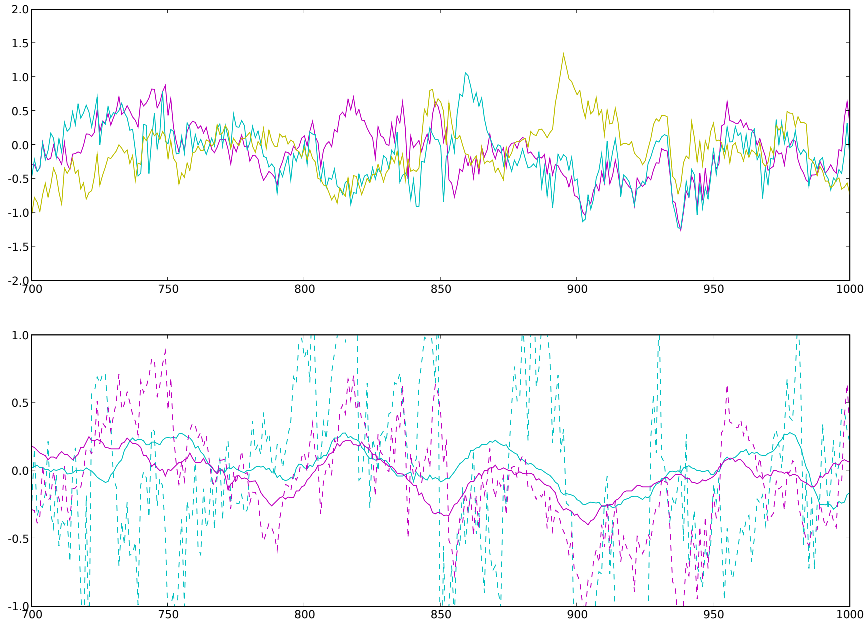

Figure 2: Fitted phases of WSRT data, see section 3.1. Top: Independent directional phases (rad) versus timestamp for 1 off center source for 3 different baselines. Bottom: Directional phases (dashed lines) and phases from the MIM model (continues lines) versus time, for 2 off center sources and 1 baseline (the purple baseline in the top picture). The phases from the MIM model are much smoother in time, because of the extra number of constraints. center source

to the 2 dimensional polynomial (or any other model). Also interesting is a plot of the phases in the direction of a gives source versus time. For this, either the calculated phases need to be stored or the coordinates of the pierce points (such that the phases can be recovered from the model and the parmdb values). This requires the possibility to store the result of the evaluation of a (sub)expression in BBS itself, which could be useful for other purposes, too. An example of such a plot is shown in Fig. 2.

2 Implementation in BBS

Here follows a short description of the implementation in BBS. For more detailed information we refer to the source code and the comments within.

The ionospheric expression is special in BBS in the sense that it uses a set of global parameters (the *MIMParms*). These parameters are the same for every station source combination, in contrast to (directional) gain parameters, which are defined *per* station (and direction). Apart from the global parameters which define our ionospheric model, we need the station coordinates and the viewing direction to calculate the phase errors for a specific station source combination. The global MIMParms as well as the azimuth/elevation nodes are defined centrally when building the calibration model including an ionospheric model.

2.1 Source code

The implementation of the ionospheric model in BBS can be found in the following sources: *MIM.cc. PiercePoint.cc, Model.cc.*

In *Model.cc* the complete expression tree is build. For the ionosphere this means the definition of the azimuth and elevation nodes and the MIMParms. Since the ionospheric model is direction dependent, one expression tree per station source combination is created. The expression tree contains one instance of a MIM node per station source combination.

PiercePoint.cc contains the code to calculate the pierce-point coordinates given a *Station* and a direction (azimuth and elevation). For every station source combination one instance of a PiercePoint node is made in the function *makeIonosphereNodes* of $Model.cc$. Apart from the x, y, z coordinates of the pierce-points, also the angle α' (equation 2) is returned as a result of the *evaluate* function[2].

MIM.cc contains the actual model. A MIM node calculates the phase correction equation 1) for a give station source combination using the values of the pierce-point coordinates, the global *MIMParms* and the coordinates of the reference pierce-point. The actual TEC model calculation is done in the function $calculate\_mim\_function$. A different model could easily be implemented by adjusting this function. For every station-source combination one instance of a MIM node is made in the function *makeIonosphereNodes* of $Model.cc$.

To use the ionospheric calibration, in the parset file set:

```
Model.Components = [IONOSPHERE]
```

One should also specify the rank of the polynomial (at least 1), by setting:

```
Model.Ionosphere.Rank = 1
```

This will create the parameters $MIM : 0 : 1, MIM : 1 : 0, \ldots, MIM : rank : rank$ for the ionospheric model. The first index refers to x, the second to y. The rank is the same for the x and y direction. To reduce the rank in one direction one can always adjust the solvability of the MIMparms.

[2] Since for every source station combination an instance of a mim node and a piercepoint node is created, they could probably be combined into 1 node. The reason to keep them into two separate classes is that in the future one might want to add different models that use piercepoints in a different way.

3 Results

3.1 Results on WSRT LFFE data

We tested the current implementation on the WSRT LFFE data set taken during 6 nights in November and December 2007. The used data was already flagged and calibrated for instrumental gains by G. Bernardi. We did repeat the calibration on part of the data as a test in BBS, but since no major differences were observed we decided to start from the corrected data.

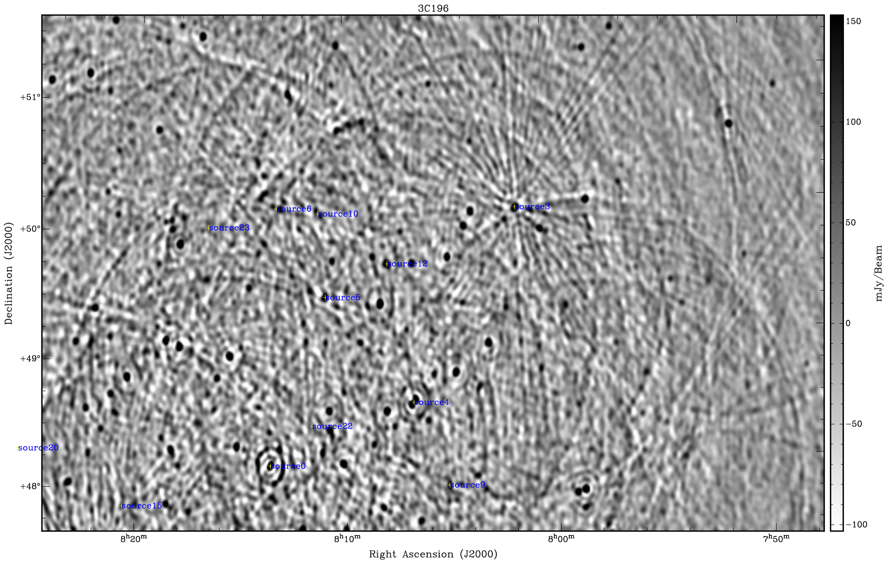

Figure 3: Residual image after first calibration, zoomed in on part of the field. The *source0* in the lower left of the image is in the center of the field. The lines around one of the brighter sources in the field (source3, upper right) are due to residual phase errors.

3.1.1 Source model

The first step for the direction dependent calibration consists of creating a source model. We used a cleaned image and the *findsources* function of the Aips++ *image* module to create the source model of all sources with a flux above a certain specified level. The MS has UVW coordinates in JAPP, but BBS assumes it to be J2000. That is the reason for a rotation of the sources. To fix this, one has to call:

```
j2convert msin=input.MS type=J2000 force=True
```

before making the image from which we extract the sources. We selected all sources with a flux higher than 0.8% of the maximum flux in the image, resulting in about 25 sources.

Findsources stores the sources in an Aips++ table. A simple python script, based on pycasa, converts this to a text file that can be read by BBS parmdb module.

3.1.2 Initial calibration

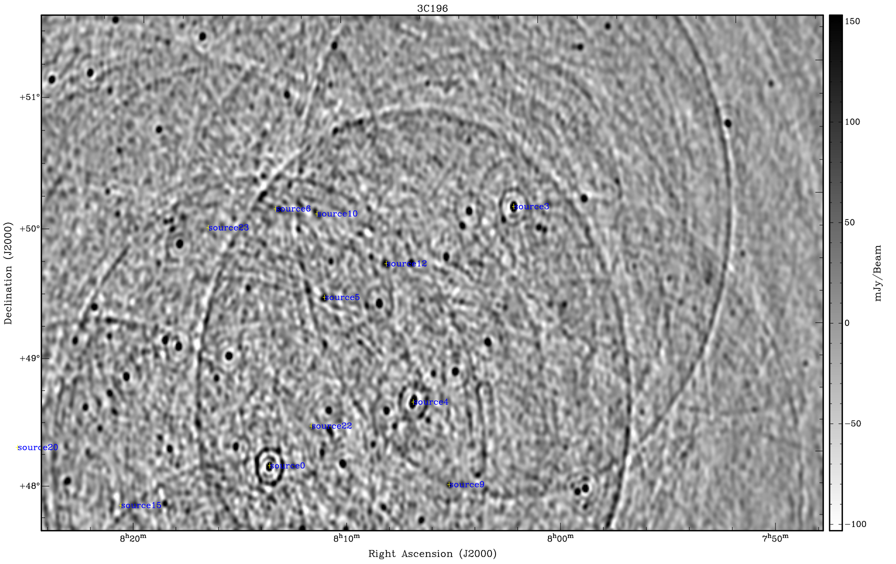

Figure 4: Residual image after calibration of directional phases in the direction of the five brightest sources. Same scale as figure 3.

The calibrated data stills shows phase errors away from the center of the field, that could point to ionospheric distortions. These size of these errors differ from night to night. We decided to focus on the data of one particularly noisy night (the 7th of December), and analyzed the first subband of this data. A residual image of this data is shown in Fig. 3, where the off center phase errors can clearly be observed.
In an initial step we use BBS to solve the directional phases of the 5 brightest sources in the field. These phases will later be compared to the results from our ionospheric model. The residual image is show in Fig 4. In this image we still see some residual flux from the subtracted sources, due to an imperfect source model. We therefore decided to redo the source finding but on an image with the five brightest sources corrected with their own phase corrections. To do this we first subtract the corrupted sources from the uv-data and in a second step add the uncorrupted model to the data. This can be done using the SUBTRACT and ADD function of BBS. In this way we are able to update our source model and redo the calibration of the directional gains. The new residual image is shown in Fig. 5. The phase solutions versus time are shown for some baselines in Fig. 2.

3.1.3 Ionospheric model

The following results are still obtained with the initial source model. A fit of the data with an updated model (as described in section 3.1.2) remains to be done.

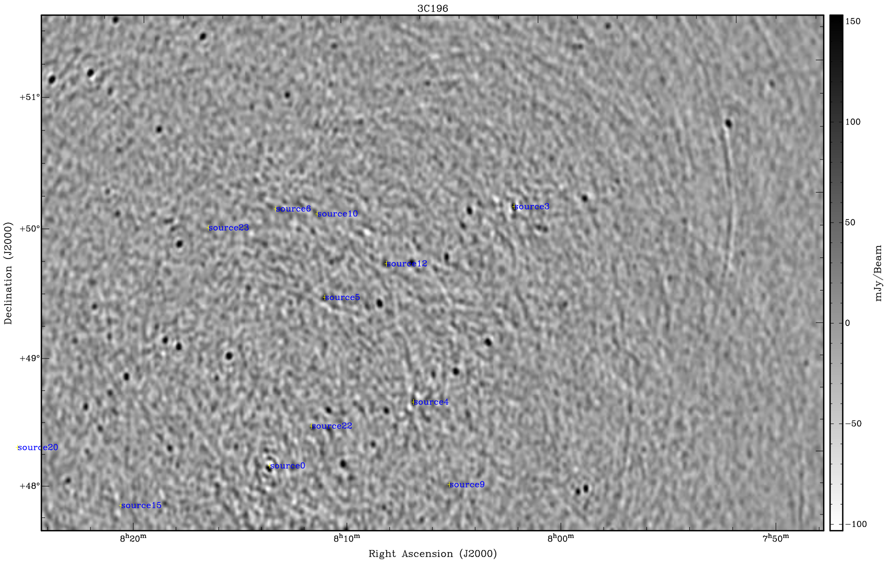

Figure 5: Residual image after calibration of directional phases in the direction of the five brightest sources, after an update of the source model (see text). Same scale as figure 3.

We obtained residual images after fitting the polynomial ionospheric model on all 25 sources in the sky model and subtracting each source with its own phase (from the ionosphere fit). In Fig. 6, 7 and 8 these images are shown for a model with 2, 5 and 8 parameters, respectively. The first two images still show residual phase errors, but after an 8 parameter fit[3] the residuals are of the same order of magnitude as in Fig. 4. However, in this case we have solutions directly for all sources in the model.

In terms of speed, the directional gain fit is a factor 2 to 4 faster. This has to do with the speed of calculating a model with more sources and could be improved if caching of the sky model is optimized.

References

[1] H.T. Intema et al. Ionospheric calibration of low frequency radio interferometric observations using the peeling scheme. to be published.

[2] J.E. Noordam et al. The MIM principle. LOFAR document, 2008.

[3] J.E. Noordam. Peeling. LOFAR document, 2002.

[3] Compare this to the 14 (antennas) times 5 (sources) parameters of the directional gain fit.

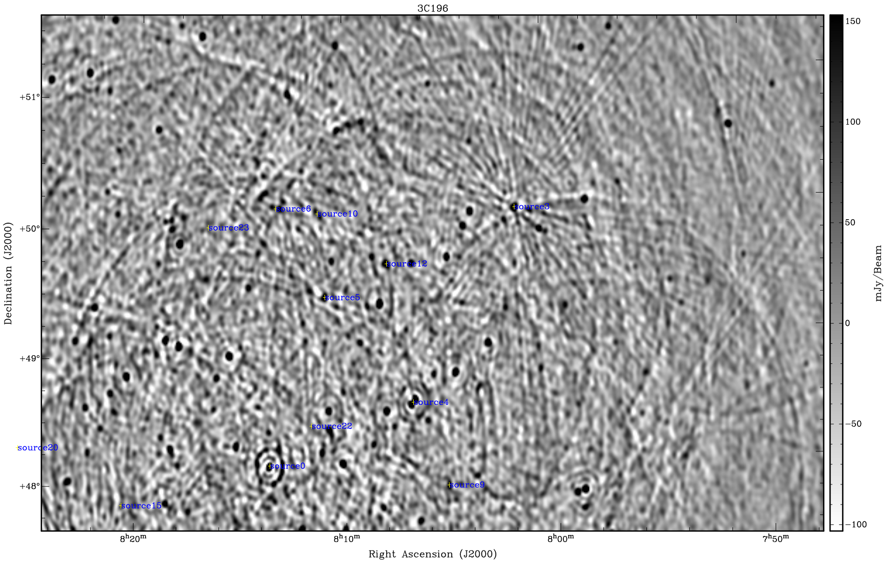

Figure 6: Residual image after calibration of a polynomial ionospheric model with 2 parameters (linear gradient only). Same scale as figure 3.

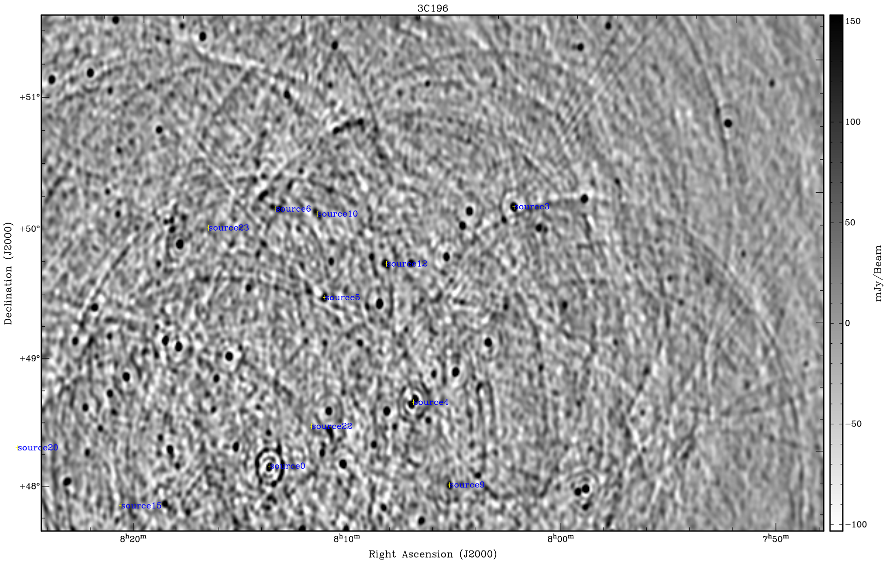

Figure 7: Residual image after calibration of a polynomial ionospheric model with 5 parameters (linear gradient and quadratic terms). Same scale as figure 3.

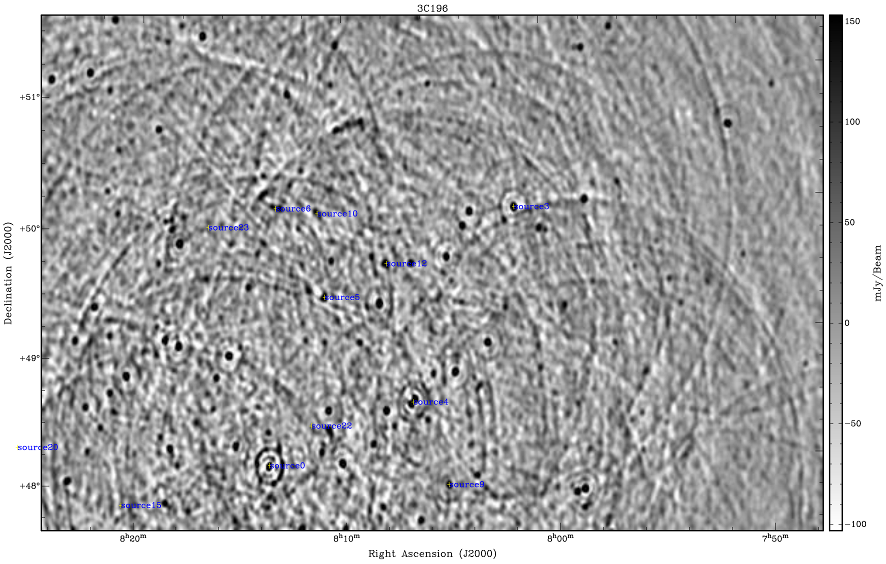

Figure 8: Residual image after calibration of a polynomial ionospheric model with 8 parameters (including third order terms). Same scale as figure 3.